Interface magnetic coupling of Fe-phthalocyanine layers on a ferromagnetic surface

E. Annese,[1,2,3] F. Casolari,[1,2] J. Fujii,[2] and G. Rossi[2,4]
[1]*Dipartimento di Fisica, Università di Modena e Reggio Emilia, via Campi 213/A, I-41100 Modena, Italy*
[2]*TASC Laboratory, IOM-CNR, SS 14, km 163.5, I-34149 Trieste, Italy*
[3]*Elettra Synchrotron S.C.p.A Trieste, SS 14, km 163.5, I-34149 Trieste, Italy*
[4]*Dipartimento di Fisica, Università degli Studi di Milano, Via Celoria 16, 20133 Milano, Italy*
(Received 16 October 2012; published 19 February 2013)

Fe-phthalocyanine (FePc) molecules bonded to metal surfaces form rehybridized interface states involving the Fe central atom reflected in changes of orbital and spin configuration. X-ray absorption spectroscopy and x-ray magnetic circular dichroism show the ferromagnetic coupling of the FePc molecules that are in contact with the Co(001) surface, even at room temperature (300 K), while the overgrown parallel layers of FePc in thicker molecular films are decoupled from the interface. The magnetized interface molecular layer reproduces the magnetic structures of the substrate (domains, patterns).

DOI: 10.1103/PhysRevB.87.054420 PACS number(s): 85.75.−d, 73.20.Hb, 75.50.Xx, 79.60.Dp

I. INTRODUCTION

Organometallic complexes form molecular superstructures on suitable templates, such as vicinal surfaces or nanostructured substrates[1,2] whose electronic properties are characteristic and represent potential building blocks for nanotechnology (e.g., gas sensors and photovoltaic cells).[3–5] In particular, for any perspective application of organic molecules in spintronics, a single organic molecule and/or molecular film with robust magnetization at and above room temperature (RT) are required. Different routes have been taken toward this goal, including the modification of the chemical structure of the molecular complex and the adsorption on suitable templates.[6–16]

The use of ferromagnetic (FM) surfaces as substrate was found to be effective in stabilizing the magnetization of metal-porphyrins, transition-metal phthalocyanine (TMPc), and single molecular magnets even at RT.[10–16] Hybrid electronic states form at the interface between a ferromagnetic surface and organic molecules. The energy alignment of the hybrid interface states with the substrate spin-polarized bands may determine spin-filtering conditions for charge transport through the interface and open a possible channel for spin injection in organic semiconducting thin films. The TMPc planar structure[10–16] and the flat absorption geometry do favor proximity between the TM centers and the surface, and spin polarization may arise in frontier orbitals originating from the macrocycles as well as from the central atom.[17,18] For instance, the spin-dependent hybridization of the macrocycle of the metal-free Pc molecule gives rise to giant magnetoresistance in a junction between the ferromagnetic surface (electrode) and the tip of a scanning tunneling microscope with a single molecule as a bridge.[19] Careful orbital configuration studies on TMPc series on ferromagnetic surfaces and spin-polarized photoemission measurements have been recently published, along with density-functional theory (DFT) calculations, yielding a general description of the phenomenology of the interaction at the molecule/ferromagnetic interface.[18] Recently, we pinpointed the relationship between the magnetic character of the molecular adlayer at the CoPc/Fe interface and its electronic properties and morphology by using x-ray absorption spectroscopy (XAS), x-ray magnetic circular dichroism (XMCD), x-ray photoemission spectroscopy (XPS), and scanning tunneling microscopy (STM).[20]

Here, we report on the study of the FePc/Co(001) interface. FePc retains a high magnetic moment upon adsorption on surfaces (higher with respect, e.g., to the CoPc molecule).[18] It was adsorbed in ultrahigh vacuum (UHV) onto the Co surface that is the most used for electrodes in spintronics application. We measured a robust magnetic coupling of the Fe(Pc) with the cobalt surface that involves changes in the iron spin and orbital moments with respect to the free-standing molecule, as monitored by the Fe $L_{2,3}$ XAS line-shape analysis and XMCD. Our data give evidence of the formation of a heterogeneous (organic/inorganic) interface that replicates the magnetization pattern of the substrate surface. This result suggests that it is, in principle, possible to design a magnetic pattern and transfer it into the organic layer that may act as a spin injector in a (homogeneous or heterogeneous) organic semiconducting film overgrown onto it.

II. EXPERIMENTAL DETAILS

The samples were prepared *in situ* (UHV) following established protocols for epitaxial growth of Co on Cu(001). 6 ML Co film (fcc) was grown *in situ* on an atomically clean Cu(001) substrate at room temperature. The Co film presents two equivalent easy magnetization axes oriented along [110] and [−110], respectively, both contained in the surface plane [Fig. 1(a)].[21] The substrate order and purity, as well as the interface morphology, were monitored *in situ* by low-energy electron diffraction (LEED) and XPS. FePc was deposited in a pressure $<4 \times 10^{-10}$ mbar and at RT: several molecular films were grown with thickness ranging from 0.5 to 3 ML. XMCD spectroscopy was exploited to probe selectively the magnetization of the substrate by measuring the Co $L_{2,3}$ transitions at 775–790 eV, and of the molecular layers by measuring the Fe $L_{2,3}$ transitions at 705–718 eV. The XMCD data were collected both in the remnant magnetization state, after saturation by an external field, and in weak applied fields to drive FM hysteresis loops [experimental geometry, Fig. 1(b)]. The magnetic order of both the substrate and the molecular overlayer were probed independently at all stages of

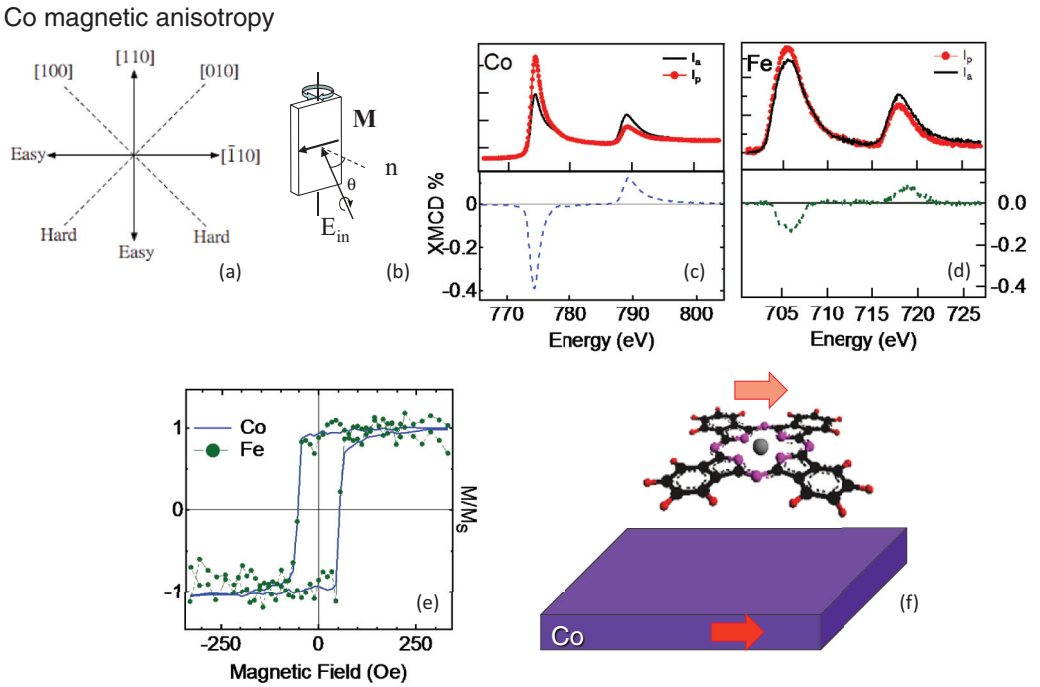

FIG. 1. (Color online) (a) The scheme illustrates the intrinsic fourfold in-plane magnetocrystalline anisotropy for a 6 ML Co film epitaxially grown on Cu(001). (b) XMCD experimental geometry with a magnetic field applied along the sample surface and circular polarized photons impinging at 60° from normal incidence. (c) Co $L_{2,3}$ and (d) Fe $L_{2,3}$ XAS spectra relative to the parallel I_p (dots) and antiparallel I_a (line) orientation of magnetization and light polarization and the relative Co and Fe XMCD spectra. (e) Element-specific hysteresis loops of Fe (dots) in the FePc molecules and Co (line) substrate obtained recording the field-dependent L_3 XMCD intensities. The hysteresis loops were normalized to the magnetization saturation values. Measurements were carried out at RT on a FePc 0.5-ML-thick molecular film. (f) Schematics of FePc and Co magnetization.

the interface growth and magnetic history. The experimental work was carried out at the APE beamline of IOM-CNR at the Elettra synchrotron radiation facility (Trieste), exploiting the UHV suite of preparation and characterization methods and the variable polarization soft x-ray for dichroism measurements.[22]

III. RESULTS AND DISCUSSIONS

Figures 1(c) and 1(d) show XAS spectra recorded at Fe and Co $L_{2,3}$ edges with photon helicity parallel I_p and antiparallel I_a to the substrate magnetization. Fe and Co $L_{2,3}$ XAS probes the unoccupied s and d states of the Fe(Pc) and the substrate as projected to the excited atom, dominated by the $2p_{1/2,3/2} \rightarrow 3d$ channel. Two groups of multiplet (broadened) peaks separated in energy by ∼13 and ∼15 eV are observed in XAS spectra for Fe(Pc) and Co respectively. The Co $L_{2,3}$ XAS spectrum is fully consistent with clean metallic cobalt at room temperature, with ∼40% XMCD on the L_3 edge and therefore high remanence.[23] The broad structured Fe $L_{2,3}$ XAS spectra of 0.5 ML FePc [Fig. 1(d)] reflect the multiplets due to the hole state configurations in the overall ligand field, whose symmetry is reduced with respect to the free molecule.

We observed a large Fe $L_{2,3}$ XMCD signal for 0.5 ML FePc film at RT, indicating that the molecules are magnetically coupled to the substrate [see the lower panel of Figs. 1(c) and 1(d), where XMCD, i.e., the asymmetry defined as $\frac{I_a - I_p}{I_a + I_p}$, is reported for Co and Fe]. The signs of Fe(Pc) and Co(substrate) XMCD agree, demonstrating that the magnetic moments of Fe (M_{Fe}) and Co (M_{Co}) are coupled parallel to each other [as represented in the schematics of Fig. 1(f)]. A finer test of the Fe(Pc) ferromagnetic coupling to the substrate can be obtained by performing full ferromagnetic hysteresis curves: Fig. 1(e) shows the hysteresis magnetization loop of the 0.5 ML FePc sample measured by recording the XMCD amplitude at Fe and Co edges as a function of applied magnetic field at RT. A square hysteresis loop with a coercive field of 50.0(5) Oe typical of epitaxial 6 ML Co film was observed. The Fe hysteresis loop overlays exactly the loop of Co, representing a full ferromagnetic coupling between M_{Fe} and M_{Co} of the substrate. The external applied field is very weak and has basically no effect on the ordering of the paramagnetic FePc molecules, as demonstrated in high-field–low-temperature studies of FePc on nonmagnetic gold surfaces when 5 T at 8 K are not sufficient to saturate the paramagnetic moments.[24–26] It is the strength of the exchange coupling at the interface, through the polarized interface states, that links the FePc first layer to the substrate, and it is the low coercivity of the cobalt substrate that allows us to trace the hysteresis in the low applied field. A similar behavior was observed in Fe-octaethylporphyrin molecules deposited on Co magnetic film.[10,13] These data give strong evidence of the formation of a hybrid organic-inorganic interface reproducing the magnetization pattern of the pristine substrate surface.

We then studied the overgrowth of further Fe(Pc) layers on top of the interface by following the evolution of Fe $L_{2,3}$ XAS and XMCD spectra [Figs. 2(a) and 1(b)] as a function

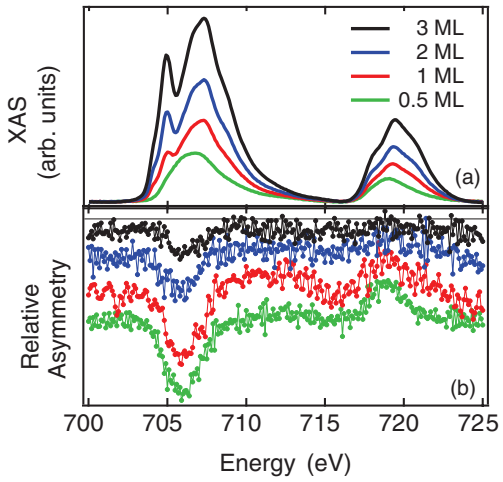

FIG. 2. (Color online) (a) Fe $L_{2,3}$ XAS spectra after background subtraction. FePc film thickness ranges from 0.5 to 3 ML from bottom to top; (b) Fe A_R spectra recorded at RT and at remanence for different coverages of FePc molecules vs FePc thickness. For the sake of clarity, the data are displayed with a vertical shift.

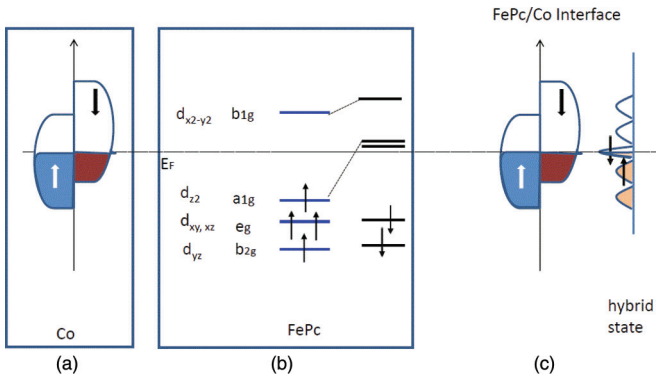

FIG. 3. (Color online) Schematics for magnetic Co (a) and freelike FePc (b) and the interface between FePc and Co (c). The schematics for freelike FePc is reproduced from Ref. 27, whereas the schematics for a hybrid state is reproduced by using XAS and XMCD experimental results and is consistent with the calculation of Ref. 18.

of molecular film thickness (0.5–3 ML). The modification of the Fe $L_{2,3}$ XAS and XMCD line shape versus FePc thickness reflects the strength of the interaction between the molecule and the substrate. The Fe $L_{2,3}$ XAS line shape reveals the electronic distribution of the FePc molecule that has a spin and orbital configuration involving d states with an out- and in-plane orbital symmetry.[24,25,27] The Fe $L_{2,3}$ XAS spectrum of 3 ML FePc shows a peak at 705.7 eV related to the a_{1g} states of d_{z^2} symmetry and the higher-energy features corresponding to the d orbital with in-plane symmetry (Fig. 2), and it is fully consistent with spectra for FePc thin films grown on different substrates and measured in cryogenic conditions.[2,24,25] The thermal broadening due to the RT measurement does not cancel the fine structure of the spectra that are dominated by the molecular states in their D_{4h} symmetry. The feature at 705.7 eV was reduced by decreasing the FePc thickness and is absent for 0.5 ML FePc film. The quenching of this feature can be related to the charge transfer from substrate to molecule.[20,24] Therefore, the XAS isotropic spectra for molecules in contact with the Co substrate are quite different with respect to those relative to the thin film.

Similar considerations can be done for the Fe $L_{2,3}$ XMCD line shape, where the data for 0.5 ML FePc show a broad weakly structured dichroic spectrum mimicking that of a metallic submonolayer, while a resolved multiplet of transitions to molecular states is reported for FePc thickness ∼1 ML on Ag or Au surfaces.[24,25] The lack of fine structure in the submonolayer and monolayer interface is not attributed to thermal broadening for $T > 80$ K, but it is interpreted as arising from a very different hybridization scheme. In the case of FePc on nonmagnetic surfaces, the charge transfer is limited to the first contact layer with two orbitals with different symmetry, carrying the magnetic moment. If we consider as a starting point the ground state, as deduced by various experimental and theoretical techniques,[28–33] i.e., $3E_g$: $(d_{xy})^2(d_{xz+zy})^3(d_{z^2})^1(d_{x^2+y^2})^0$ (see Fig. 3), the empty Fe d states that interact with the substrate and are involved in the rehybridization process are the singlet d_{z^2} and d_{xz},d_{yz}. In the present case, the hybridization involves the broad spin-polarized 3d band of the cobalt substrate, with a high density of states at the Fermi level, rather than the s-p extended states of Au or Ag. Figure 3 displays a schematic of the FePc/Co interface in terms of intermixing between molecule and substrate. This representation about the interface accounts for the experimental evidence, i.e., the broadening [exaggerated in Fig. 3(c)] of the molecular states due to the hybridization with the substrate, and the molecular energy level shift corresponding to the disappearance of the a_{1g} feature in Fe L_3 spectra at FePc thickness ∼1 ML. The schematics is also in agreement with the DFT calculations in Ref. 18, which indicate a rehybridization of the Fe(Pc) orbital when the Fe ion sits on a bridge position between two surface Co atoms at an Fe-Co distance of 0.224 nm.

To analyze the Fe magnetic signal, we define the magnetic asymmetry (A_M) as obtained normalizing the iron XMCD signal (I_a-I_p) to the area of the cobalt dichroic spectrum. This is useful to disentangle the FePc magnetic signal from the underlying substrate domain structure. A_M is proportional to the overall magnetization of Fe atoms within the molecular film. We further define the relative asymmetry (A_R) as A_M normalized to Fe isotropic intensity to obtain a signal proportional to the number of magnetic molecules per total number of molecules. The XMCD data in Fig. 2(b) are displayed normalized as A_R and show that the magnetic signal of Fe(Pc) atom scales with the coverage, being minimal for 3 ML. From the comparison of Fe L_3 integrated A_M and A_R versus FePc thickness, reported in Fig. 4, we can evaluate the molecular layers that contribute to the magnetic coupling. A_M grows at submonolayers and then remains constant for FePc thickness greater than or equal to 1 ML, whereas A_R intensity decreases for films thicker than 1 ML, giving a clear indication that the Fe magnetic signal originates entirely from FePc molecules at the interface with Co, with no contributions from the overlayer molecules. The noninterface molecules are therefore in the paramagnetic state and require a strong applied film to be oriented as expected because a thin layer of FePc stacking parallel to metal substrates has exhibited

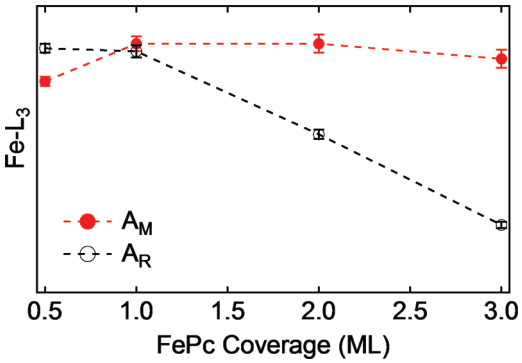

FIG. 4. (Color online) Fe L_3 integrated magnetic asymmetry (filled circles) and relative asymmetry (empty circles) vs FePc thickness.

in-plane anisotropy in previous studies.[26] Cooling the sample down to 80 K (LT) did not increase the dichroic signal as shown in Fig. 5(a), where Fe A_R spectra at RT and LT of 1 ML FePc are displayed. This indicates an exchange coupling between FePc and Co substrate, whose energy is much greater than the thermal reduction of magnetic order in the molecules.

Hereafter, we highlight how effective the magnetic coupling is between the molecule and the substrate, irrespective of the complex magnetic reversal process within the substrate. To this end we exploit the temperature-dependent Fe and Co hysteresis loops at 80 K measured on a different 0.5 ML FePc sample. In Figs. 5(b)–5(e), the hysteresis loops at the Co and Fe L_3 edges measured at LT and RT are reported. The RT Co hysteresis loop for this sample is not squared, even though it corresponds to the same nominal Co film thickness. Similar hysteresis loop shapes are commonly observed in the case of a miscut of Cu substrates as well as for incomplete or textured Co layers, for off-normal deposition geometry from the sample surface, and when nanostructuring occurs due to ion bombardment.[21,34–36] Our Co film showed a sharp low-energy electron diffraction pattern signature of the structural coherence of large single-crystal domains. Therefore, the strain in the substrate manifests itself in the complex shape hysteresis loops due to the competing in-plane anisotropies. The substrate strain may change, nevertheless, from one preparation to the other (implanted Ar during sputtering, different temperature gradients during annealing), giving rise to the complex-shape hysteresis loops that reflect the competing in-plane anisotropies allowed on Co(001) (inset of Fig. 5). By lowering the temperature, we measure a slight increase in the magnetization saturation value of Co (by $\sim 6\%$) and in a coercive field (from 44 to 55 Oe), as expected in relation to thermal-activated domain-wall motion. The same increase in amplitude was measured in the FePc hysteresis loops [Figs. 5(a) and 5(b)] where the intensity of the hysteresis is not normalized for the magnetization saturation value. The M_{Fe} signal varies with temperature because it follows the variation of the underlying M_{Co}. This result further confirms the strong magnetic coupling between Fe(Pc) and Co, and it

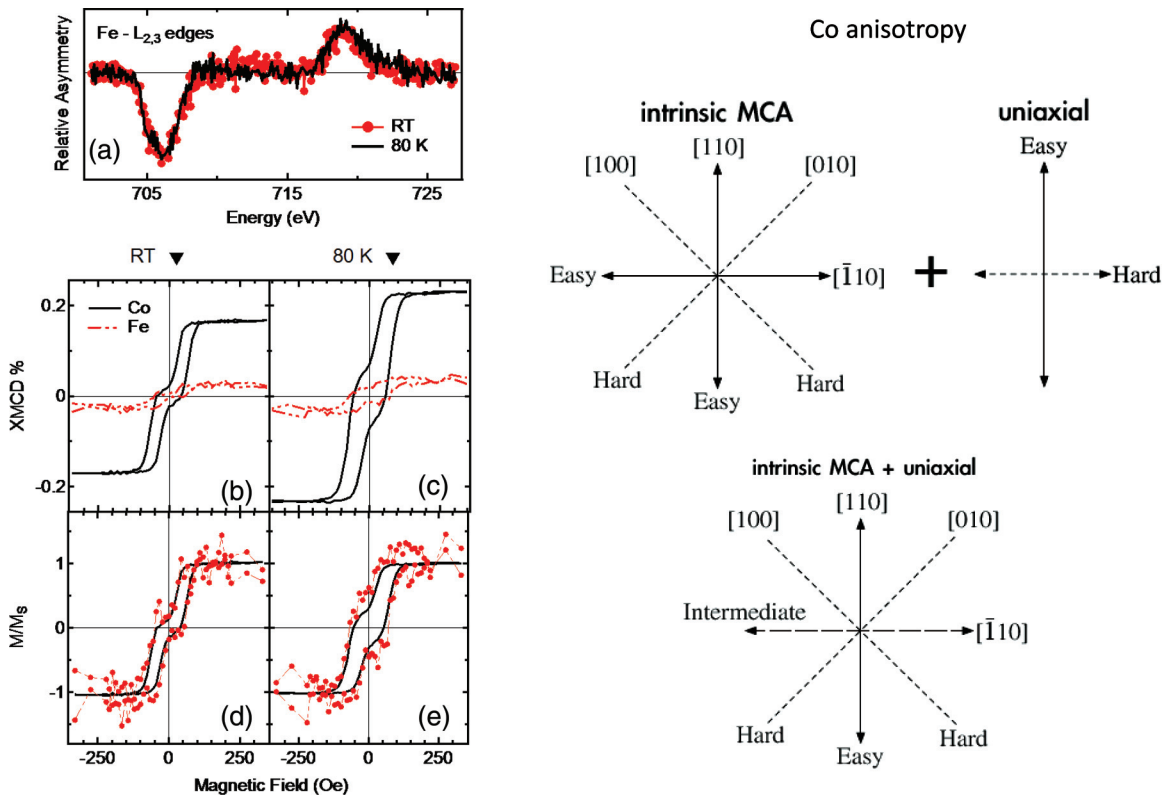

FIG. 5. (Color online) (a) Fe $L_{2,3}$ A_R spectra recorded at RT (solid line) and at 80 K (dotted line) for 1 ML FePc. Right: (b)–(e) Element-specific field-dependent L_3 XMCD percentage intensities and normalized hysteresis loops at Fe L_3- (dotted line) and Co L_3-edge (solid line). Left: Effect of the morphology-induced in-plane uniaxial anisotropy term: [110] and [−110] crystallographic directions are not equivalent.

TABLE I. Fe(Pc) $m^{\parallel}_{S\text{eff}}$ and $m^{\parallel}_{L}$ of a molecular single crystal or molecule interacting with different surfaces.

FePc (thickness)	Substrate	T (K)	$m^{\parallel}_{S\text{eff}}$ (μ_B)	$m^{\parallel}_{L}$ (μ_B)
0.5 ML	Co	300	0.52(2)	0.039(1)
crystal α-phase[25]	Au	6	0.90(6)	0.53(4)
5×3 reconstruction[26]	Au(110)	6	0.14(3)	0.09(1)

determines that it is feasible to control the magnetization of a molecule by engineering the substrate magnetization.

To evaluate the effect of the molecule/substrate interaction on the magnetic moment of the Fe(Pc) atom, we estimated the Fe effective spin ($m_{S\text{eff}}$) and orbital magnetic (m_L) moment of FePc/Co through XMCD sum rules[28,37] using as the number of hole $n_h = 2.669$ the one calculated by Kuz'min *et al.* in Ref. 27. In the present case, we explored Fe(Pc) m_L and $m_{S\text{eff}}$ in the surface plane (xy). Upon adsorption on metal surfaces, both $m^{\parallel}_{S\text{eff}}$ and $m^{\parallel}_{L}$ of Fe(Pc) reduce with respect to those of FePc in the crystal α phase, as shown in Table I, where Fe(Pc) moments are reported for FePc α-crystal,[25] FePc/Co, and FePc/Au (Ref. 26) interfaces. Although $m^{\parallel}_{S\text{eff}}$ and $m^{\parallel}_{L}$ of Refs. 25 and 26 are underestimated because the molecules are not fully aligned, i.e., the maximum field and the lowest temperature do not saturate the Fe(Pc) magnetization, it is worthwhile to compare the different behavior of Fe(Pc) in these different cases. Fe(Pc) α-crystal presents highly unquenched $m^{\parallel}_{L}$, whereas both interfaces show $m^{\parallel}_{L}$ mainly quenched, indicating Fe(Pc) $3d$ states at the interface are more delocalized or hybridized with respect to those of FePc crystal or a single Fe adatom. On the other hand, Fe(Pc) $m^{\parallel}_{S\text{eff}}$ is mainly reduced at FePc/Au. If we assume that at the submonolayer coverage all FePc molecules lay flat and are coupled to the substrate, the magnitude of the Fe(Pc) XMCD asymmetry is a direct measure of M_{Fe} with an Fe(Pc) effective in-plane magnetic moment of $0.56(2)\mu_B$. This is a sizable magnetic moment, definitely larger than for Fe(Pc) on noble metal surfaces, as a consequence of the hybridization with the spin-polarized states of the Co surface, but smaller than the magnetic moment M_{Fe} of $1.06\mu_B$ estimated in FePc paramagnetic thin films.[24] A large M_{Fe} (e.g., $1.94\mu_B$) was also predicted by DFT calculation[18] for the adsorbed Fe(Pc) molecule on bridge sites on the Co surface.

The spin in the ground state of FePc has an important role in determining the properties of Fe(Pc) in contact with Co. Further experimental information can be retrieved from the analysis of the intensity ratio of the L_3 and L_2 white-line edge spectra in XAS: the branching ratio $B = I(L_3)/[I(L_2) + I(L_3)]$ is directly proportional to the expectation value of the angular part Z of the spin-orbit operator, $B = \frac{2}{3} - \frac{1}{3n_h}Z$, in the case of the $2p^6 3d^n \rightarrow 2p^5 3d^{n+1}$ transition.[37–39] The Fe $L_{2,3}$ isotropic XAS spectrum of 0.5 ML FePc shows a branching ratio of 0.74(2) that deviates from the statistical value of 2/3. A similar deviation from the statistical value has been observed in CuPc adsorbed on Ag(100) (Ref. 24), but it was associated with a robust spin and the orbital local magnetic properties at the interface.

IV. CONCLUSIONS

We have obtained clear evidence that FePc molecules couple ferromagnetically with the cobalt surface at room temperature. The rehybridization of the molecular states corresponds to a filling of the molecular d_{z^2} states (a_{1g}) which reduces the molecule magnetic moment. The mixing of the planar d states with the spin-polarized states of the substrate effectively locks in the molecular magnetization parallel to the substrate surface. The exchange coupling is very robust, showing FePc XMCD values much larger than for FePc on gold surfaces in a 5 T field, and is only slightly affected by temperature between 80 and 300 K. The magnetic coupling is confined at the interface between Fe(Pc) and Co. The magnetic pattern of the substrate, e.g., magnetization reversal loops, is directly mapped into the magnetic pattern of the interface molecules. The molecules appear to be individually coupled to the substrate and weakly coupled among them, allowing, in principle, for nanometric magnetic patterning of the substrate and consequent replica patterning in the molecular interface layer acting as a spin injector in the organic overlayer. Exploiting the spin-polarized interface states may lead to controlled spin injection currents in organic semiconducting layers.

ACKNOWLEDGMENTS

E.A. would like to acknowledge R. Moroni and F. Bisio for fruitful discussions. This work was carried out in the framework of the PRIN 2008 525SC7 contract coordinated by M. G. Betti. This work was also supported by the NFFA project (WWW.NFFA.eu).

[1] T. Gredig, C. N. Colesniuc, S. A. Crooker, and I. K. Schuller, Phys. Rev. B **86**, 014409 (2012).
[2] M. G. Betti, P. Gargiani, R. Frisenda, R. Biagi, A. Cossaro, A. Verdini, L. Floreano, and C. Mariani, J. Phys. Chem. C **114**, 21638 (2010).
[3] S. R. Forrest, Chem. Rev. **97**, 1793 (1997).
[4] V. A. Dediu, L. E. Hueso, I. Bergenti, and C. Taliani, Nat. Mater. **8**, 707 (2009).
[5] S. Heutz, C. Mitra, W. Wu, A. Fisher, A. Kerridge, M. Stoneham, A. Harker, J. Gardener, H.-H. Tseng, T. Jones, C. Renner, and G. Aeppli, Adv. Mater. **19**, 3618 (2007).
[6] P.-H. Lin, T. Burchell, L. Ungur, L. Chibotaru, W. Wernsdorfer, and M. Murugesu, Angew. Chem. **121**, 9653 (2009).
[7] S. Takamatsu, T. Ishikawa, S. Koshihara, and N. Ishikawa, Inorg. Chem. **46**, 7250 (2007).
[8] M. Mannini, F. Pineider, P. Sainctavit, C. Danieli, E. Otero, C. Sciancalepore, A. M. Talarico, M.-A. Arrio, A. Cornia, D. Gatteschi, and R. Sessoli, Nat. Mater. **8**, 194 (2009).
[9] P. Gambardella, S. Stepanow, A. Dmitriev, J. Honolka, F. M. F. de Groot, M. Lingenfelder, S. S. Gupta, D. D. Sarma, P. Bencok, S. Stanescu, S. Clair, S. Pons, N. Lin, A. P. Seitsonen, H. Brune, J. V. Barth, and K. Kern, Nat. Mater. **8**, 189 (2009).

[10]H. Wende, J. Luo, C. Sorg, N. Ponpandian, J. Kurde, J. Miguel, J. Miguel, M. Piantek, X. Xu, P. Eckhold, W. Kuch, K. Baberschke, P. M. Panchmatia, B. Sanyal, P. M. Oppeneer, and O. Eriksson, Nat. Mater. **6**, 516 (2007).
[11]A. Scheybal, T. Ramsvik, R. Bertschinger, M. Putero, F. Nolting, and T. Jung, Chem. Phys. Let. **411**, 214 (2005).
[12]T. Suzuki, M. Kurahashi, and Y. Yamauchi, J. Phys. Chem. B **106**, 7643 (2002).
[13]M. Bernien, X. Xu, J. Miguel, M. Piantek, P. Eckhold, J. Luo, J. Kurde, W. Kuch, K. Baberschke, H. Wende, and P. Srivastava, Phys. Rev. B **76**, 214406 (2007).
[14]S. Javaid, M. Bowen, S. Boukari, L. Joly, J.-B. Beaufrand, X. Chen, Y. J. Dappe, F. Scheurer, J.-P. Kappler, J. Arabski, W. Wulfhekel, M. Alouani, and E. Beaurepaire, Phys. Rev. Lett. **105**, 077201 (2010).
[15]Y. Zhan, E. Holmstrm, R. Lizrraga, O. Eriksson, X. Liu, F. Li, E. Carlegrim, S. Stafstrm, and M. Fahlman, Adv. Mater. **22**, 1626 (2010).
[16]A. Lodi-Rizzini, C. Krull, T. Balashov, J. J. Kavich, A. Mugarza, P. S. Miedema, P. K. Thakur, V. Sessi, S. Klyatskaya, M. Ruben, S. Stepanow, and P. Gambardella, Phys. Rev. Lett. **107**, 177205 (2011).
[17]S. Sanvito, Nat. Phys. **6**, 562 (2010).
[18]S. Lach, A. Altenhof, K. Tarafder, F. Schmitt, M. E. Ali, M. Vogel, J. Sauther, P. M. Oppeneer, and C. Ziegler, Adv. Funct. Mater. **22**, 989 (2012).
[19]S. Schmaus, A. Bagrets, Y. Nahas, T. K. Yamada, A. Bork, M. Bowen, E. Beaurepaire, F. Evers, and W. Wulfhekel, Nat. Nanotech. **6**, 185.
[20]E. Annese, J. Fujii, I. Vobornik, G. Panaccione, and G. Rossi, Phys. Rev. B **84**, 174443 (2011).
[21]S. van Dijken, G. Di Santo, and B. Poelsema, Phys. Rev. B **63**, 104431 (2001).
[22]G. Panaccione, I. Vobornik, J. Fujii, D. Krizmancic, E. Annese, L. Giovanelli, F. Maccherozzi, F. Salvador, A. D. Luisa, D. Benedetti, A. Gruden, P. Bertoch, F. Polack, D. Cocco, G. Sostero, B. Diviacco, M. Hochstrasser, U. Maier, D. Pescia, C. H. Back, T. Greber, J. Osterwalder, M. Galaktionov, M. Sancrotti, and G. Rossi, Rev. Sci. Instrum. **80**, 043105 (2009).
[23]C. T. Chen, Y. U. Idzerda, H.-J. Lin, N. V. Smith, G. Meigs, E. Chaban, G. H. Ho, E. Pellegrin, and F. Sette, Phys. Rev. Lett. **75**, 152 (1995).
[24]S. Stepanow, P. S. Miedema, A. Mugarza, G. Ceballos, P. Moras, J. C. Cezar, C. Carbone, F. M. F. de Groot, and P. Gambardella, Phys. Rev. B **83**, 220401 (2011).
[25]J. Bartolomé, F. Bartolomé, L. M. Garcia, G. Filoti, T. Gredig, C. N. Colesniuc, I. K. Schuller, and J. C. Cezar, Phys. Rev. B **81**, 195405 (2010).
[26]P. Gargiani, G. Rossi, R. Biagi, V. Corradini, M. Pedio, J. C. Cezar, N. B. Brookes, and M. G. Betti (unpublished).
[27]M. D. Kuz'min, R. Hayn, and V. Oison, Phys. Rev. B **79**, 024413 (2009).
[28]P. Carra, B. T. Thole, M. Altarelli, and X. Wang, Phys. Rev. Lett. **70**, 694 (1993).
[29]M. Evangelisti, J. Bartolomé, L. J. de Jongh, and G. Filoti, Phys. Rev. B **66**, 144410 (2002).
[30]M.-S. Liao and S. Scheiner, J. Chem. Phys. **114**, 9780 (2001).
[31]C. G. Barraclough, R. L. Martin, S. Mitra, and R. C. Sherwood, J. Chem. Phys. **53**, 1638 (1970).
[32]P. Coppens, L. Li, and N. J. Zhu, J. Am. Chem. Soc. **105**, 6173 (1983).
[33]W. Junhua, S. Yisheng, C. Juexian, and W. Ruqian, Appl. Phys. Lett. **94**, 122502 (2009).
[34]R. A. Hyman, A. Zangwill, and M. D. Stiles, Phys. Rev. B **58**, 9276 (1998).
[35]R. Moroni, F. Bisio, F. Buatier de Mongeot, C. Boragno, and L. Mattera, Phys. Rev. B **76**, 214423 (2007).
[36]D. Sekiba, R. Moroni, G. Gonella, F. B. de Mongeot, C. Boragno, L. Mattera, and U. Valbusa, Appl. Phys. Lett. **84**, 762 (2004).
[37]B. T. Thole, P. Carra, F. Sette, and G. van der Laan, Phys. Rev. Lett. **68**, 1943 (1992).
[38]B. T. Thole and G. van der Laan, Phys. Rev. B **38**, 3158 (1988).
[39]G. van der Laan and B. T. Thole, Phys. Rev. Lett. **60**, 1977 (1988).